JOURNAL OF MATERIALS SCIENCE 23 (1988) 145–149

Thickness dependence of H_2 gas sensor in amorphous SnO_x films prepared by ion-beam sputtering

TAKEYUKI SUZUKI, TSUTOMU YAMAZAKI, HIROSHI YOSHIOKA, KUNIYUKI HIKICHI
Department of Industrial Chemistry, Tokyo University of Agriculture and Technology, Koganeishi, Tokyo 184, Japan

Amorphous SnO_x films were deposited by ion-beam sputtering on sintered alumina substrates. Amorphous film sensors were prepared by annealing the films at 300° C for 2 h in air. The thickness dependence of resistivity and hydrogen gas sensitivity were measured at 150° C over the thickness range ~1 to 700 nm. A resistivity maximum was observed in ultrathin films. Resistivity increased by three orders of magnitude with increasing film thickness from 0.9 to 7.4 nm and then decreased by five orders of magnitude from 7.4 to 35 nm. Ultrathin film sensors showed sensitivity maxima around a thickness of 10 nm. Sensitivity and resistivity of ultrathin films were significantly influenced by the thermal expansion coefficient and the surface state of the substrate.

1. Introduction

Since the pioneering work of Seiyama *et al.* [1], semiconductor gas sensors have been extensively studied for their wide applications. The gas sensor characteristics of n-type semiconductors SnO_x depend greatly on the geometrical factors of films or sintered porous bodies. Sakai *et al.* [2] have theoretically analysed the effects of film thickness on the sensor properties. On the basis of surface-controlled conduction in homogeneous semiconductors, they concluded that the resistivity was surface controlled for films thinner than the Debye length, L_D; for films thicker than $3L_D$, the resistivity was controlled by the bulk. The thickness dependence of electrical properties of undoped- and doped-SnO_x films has been reported. For example, Vossen and Poliniak [3] have deposited antimony-doped SnO_2 films by r.f. sputtering. Films were annealed at 300° C for 15 min in air. They observed that the resistivity of thicker films (40 to 100 nm) was independent of thickness; however, a noticeable increase occurred at thickness less than 30 nm and continued increasing down to 5 nm. Pink *et al.* [4] have deposited films (20 to 100 nm) by spray pyrolysis on quartz and Al_2O_3–ceramic substrates. Although these films resulted in fast and sensitive sensors, the dependence of sensor properties on the film thickness was not reported. Kaneko and Miyake [5] have prepared antimony-doped SnO_2 films by a chemical spray deposition method on different glass substrates held at 600° C. The films were 100 to 1400 nm thick. They found that the resistivity of the films on fused quartz and borosilicate glass substrates were independent of the film thickness. Films thicker than 400 nm on soda–lime glass substrate had an almost constant resistivity, although a large increase in resistivity of thinner films was observed. The properties of the films on soda–lime glass substrate were thought to be caused by an active component in the substrate material, especially in thin films. Bélanger *et al.* [6] have deposited antimony- and fluorine-doped SnO_2 films (≈ 200 to 5500 nm thick) by CVD on borosilicate and silica substrates. For films thinner than 1000 nm, resistivity increased with decreasing film thickness; above 1000 nm the resistivity remained constant. Dibbern *et al.* [7] have prepared SnO_x films by cathode sputtering on oxidized silicon wafers. Films were annealed at 300 to 500° C for 12 to 65 h. They reported that the film thickness (100 to 1500 nm) had no influence on hydrogen gas sensitivity or resistivity and that good gas sensitivity was found only with low deposition rates (less than 3 nm min^{-1}).

Grisel and Demarne [8] have deposited films by magnetron sputtering on quartz. The carbon monoxide gas sensor characteristics of these films were studied after annealing the films at 350° C for 7 h in air. The resistance increased by one to four orders of magnitude as the thickness decreased from 73 to 35, 31 and 27 nm. However, no clear correlation could be established between the film thickness and the gas sensing.

Apart from these films, sensor properties of whiskers and ultrafine particle films have also been reported. Egashira *et al.* [9] have grown SnO_2 whiskers (0.7 to 31.3 μm thick and 7.1 to 68.6 μm wide) by oxidation of metallic tin at 1100° C under low partial pressure of oxygen. They observed no correlation between gas sensitivity and whisker thickness. They noted that all the whiskers which were highly gas sensitive showed very rough surfaces or included crystallographically higher index planes. Ogawa *et al.* [10] have prepared ultrafine particle films by evaporating Sn, SnO and SnO_2 under low oxygen pressure on

0022–2461/88 $03.00 + .12

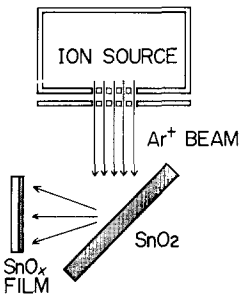

Figure 1 A schematic illustration of the ion-beam sputtering.

silica and silicon covered with SiO_2. Mean particle size (≈ 1 to 20 nm) could be increased by increasing the oxygen pressure (0.05 to 10 torr). The resistance of these porous films increased sharply as the thickness decreased. They postulated that this sharp increase was due to discontinuities in ultrafine particle films at the initial stage of the growth on the substrate. The sensitivity was strongly related to the composition, mean particle size and the structure of the films. A number of other topics relating to the SnO_2 conductors have already been fully reviewed by Chopra *et al.* [11].

In none of these investigations, except the work on whiskers, were the effects of grain boundary and film thickness separated. The present investigation was undertaken to determine clearly the thickness dependence of gas sensor properties. To exclude the grain boundaries, amorphous SnO_x films were examined.

2. Experimental methods

Samples were prepared using an ion-beam sputtering (IBS) apparatus. The principle of IBS is shown schematically in Fig. 1. The IBS system was evacuated to $< 2 \times 10^{-5}$ torr and subsequently argon gas was fed into the apparatus which gave a chamber pressure of (1.0 to 1.2) $\times 10^{-4}$ torr during sputtering. Electrode formation was carried out first. Platinum was sputtered on a substrate (6 mm $\times$ 12 mm) covered with a hard mask of metal plate (0.5 mm wide) or metal wires (120 and 40 μm diameter). This resulted in the electrode gap of 455 $\pm$ 5, 80 $\pm$ 20, and 15 $\pm$ 5 μm, respectively. Then SnO_x films (6 mm $\times$ 7 mm) were deposited by sputtering the disc-shaped 99.99% pure SnO_2 target (High Purity Chemical Lab.) using a 1 kV and 3.5 to 4.0 mA beam. Sputtering time ranged from 9 sec to 4 h. The target was placed on a water-cooled copper plate. The substrate was held 7 cm from the target; the substrate temperature did not exceed 65° C in 2 h. Details of the IBS apparatus have been published elsewhere [12]. Five different substrates were used; they were optically flat quartz and Pyrex glasses, sintered alumina (Furuuchi Chemicals), sintered mullite and sintered magnesia. Mullite and magnesia were cut from ceramic tubes, therefore their surfaces were very rough. Substrates were washed with acetone prior to sputtering. The thickness of deposited films was measured with a surface texture measuring instrument (Ferfcom, Tokyo Precision). The film structure was studied using X-ray diffraction with 30 kV–20 mA Cu$K\alpha$ radiation (RAD-B, Rigaku). The intensity data were collected with a scan

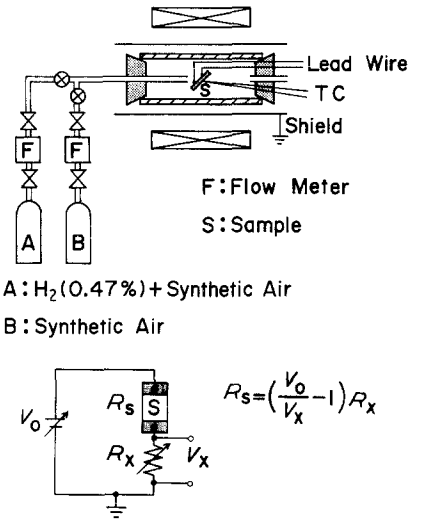

Figure 2 Measurement system for sensor properties.

speed of 0.1° min^{-1} and a step sampling of 0.002° in 2θ. All samples were annealed at 300° C for 2 h in air. Fig. 2 shows the experimental arrangement for sensor properties. The functions of various elements shown in the diagram are self-explanatory. Throughout the experiments, the sensor temperature was kept at 150° C. Synthetic air (s-air) constituents were comprised of: 20.7% O_2, 0.1% > CO_2, 0.1 p.p.m. > CH_4; balance N_2. The gas flow rate was set to 50 ml min^{-1}. Electrical contacts were made with 0.5 mm silver wire pressure-contacted to the platinum electrodes. The contact resistance between wires and electrodes and the internal resistance of the d.c. generator (TR-6141, Advantest) were sufficiently small compared with the film resistance. Applied voltage, V_0, was regulated so that the current density through the film just before the first introduction of hydrogen gas was 200 mA cm^{-2}. When the film resistance was too high to maintain the desired current density, electrical properties were measured with $V_0 = 10$ V, i.e. with a lower current density. The gas sensitivity was defined as the ratio of the resistance in s-air (R_0) to that in 0.47% H_2 (R_g). A film is specified by its sputtering time, t, and the electrode gap, d. We will abbreviate this to (t, d) or simply (t) here.

3. Results and discussion

3.1. Film thickness and structure

The thickness of as-deposited films obtained by sputtering for 2 h was 350 nm. Thus the deposition rate was 0.049 nm sec^{-1}. The thickness of all other films was calculated from this rate. Because factors affecting the deposition rate, such as argon pressure, beam power and target temperature (< 230° C), remained almost constant, this estimation of film thickness is a good approximation. Fig. 3 shows the X-ray diffraction diagram of the deposited films before and after annealing. As-deposited film shows only broad amorphous haloes, whereas annealed film shows a very small crystalline peak at $2\theta = 31.6°$. The structure of this small amount of crystals was found to be the trigonal Sn_3O_4 (JCPDS 20-1293). Thus annealed films are almost amorphous, therefore one can neglect the formation of grain boundaries.

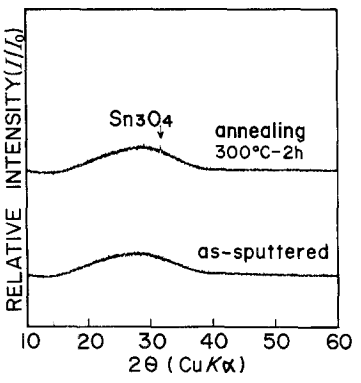

Figure 3 X-ray diffraction diagram of films. Film thickness = 350 nm.

3.2. Sensitivity

As a typical example, the response of the film (3 min, 455 μm) to hydrogen gas is shown in Fig. 4. The first peak occurs when the ordinary air is replaced by the s-air. Because the ordinary air contains extra H_2O, the first small peak corresponds to the desorption of H_2O and the subsequent adsorption of oxygen. Under four continuous measurements the hydrogen sensitivity decreased from 5.5 to 4.5, 4.5 and finally to 4.3. 90% rise time at the first response was 100 sec. Similarly all films on alumina substrates were examined.

Sputtering time dependence of sensitivity is clearly demonstrated in Fig. 5. We see three distinct regions according to the sputtering time or the film thickness, L: (1) high stability and low sensitivity for $t > 400$ sec ($L > 20$ nm); (2) high sensitivity and low stability for 100 sec $< t <$ 400 sec (5 nm $< L <$ 20 nm); (3) low sensitivity and low stability for $t <$ 100 sec ($L <$ 5 nm). Thinner films ($L <$ 5 nm) usually showed a peculiar behaviour; sensitivity was less than unity. This is due to an increase in resistance at the first introduction of hydrogen. Once increased, the resistance remained nearly constant on introduction of another gas. Probably the response time against the change from hydrogen to s-air is very long. For thicker films ($L >$ 20 nm) no dependence of sensitivity on the electrode gap was observed. This is natural because SnO_x films were amorphous and homogeneous. However, high sensitivity films (5 nm $< L <$ 20 nm) behaved differently. Contrary to our expectation, in four films out of five, sensitivity depended on the electrode gap. Therefore our next step was to enquire into the electric field effect. This was done by changing the voltage by several orders. Fig. 6 compares the sensitivity of the films (3 min, 455 μm, and 3 min, 80 μm) as a function of applied voltage. Here again the gap effect on sensitivity appeared. Further, another film (3 min, 15 μm) was prepared; its sensitivity was found to lie between 1.0 and 1.1 for a wider voltage range of 10 mV to 10 V. Thus we conclude that a wider electrode gap or probably a larger gap area is preferable for a higher sensitivity in amorphous films. It is to be noted that sensitive films tended to be more sensitive after a few days. So far, we have not referred to the sensitivity maxima around the film thickness of 10 nm. This is dealt with indirectly in the next section.

3.3. Resistivity

Fig. 7 shows the film resistivity in s-air as a function of sputtering time. Resistivity was calculated from the film thickness, electrode gap (455 and 80 μm), electrode width (6 mm) and the resistance just before the first introduction of hydrogen in the same series of experiments described above. The figure presents two outstanding features; a sharp increase and a steep decrease in resistivity with the sputtering time for 18 sec $< t <$ 12 min. As far as we are aware, observations similar to the increase in resistivity by three orders of magnitude from 18 sec to 153 sec, 80 μm have never been reported. Resistivity is approximately proportional to $L^{5/2}$ within the thickness range 1.7 to 7.4 nm. For thicker films up to 35 nm, a decrease in resistivity by five orders of magnitude is seen. Qualitatively, a similar reduction is generally observed in many films [3, 5, 6, 8, 11].

According to the theoretical analysis of Sakai *et al.* [2], resistivity of n-type crystalline semiconductors is inversely proportional to the film thickness when the film thickness is less than the Debye length. The present investigation on amorphous films shows, however, that the resistivity is approximately proportional to L^{-10} in the thickness range 7.4 to 17 nm. Let us now relate the resistivity with the sensitivity.

These phenomena are quite strongly interrelated, leading to a crude conclusion that a high sensitivity arises from a high resistivity near the resistivity maximum. This finding of a resistivity maximum led us to investigate the carrier species. A preliminary measurement on the sign of the Seebeck coefficient [13] revealed: (1) films thicker than 10 nm were electron conductors; (2) thinner films, (3 min, 455 μm, and 153 sec, 455 μm), exhibited evidence of hole conductors. Other films near the resistivity maximum were not stable and the sign changed with time, generally from plus to minus. Thus we are ready to postulate that a high sensitivity arises from the formation of an inversion layer [14] in ultrathin amorphous films and that this change increases the resistivity first and then decreases it, exhibiting the resistivity maximum. It is to be noted that the properties of the two films 126 sec, 455 μm and 153 sec, 455 μm, were examined with a

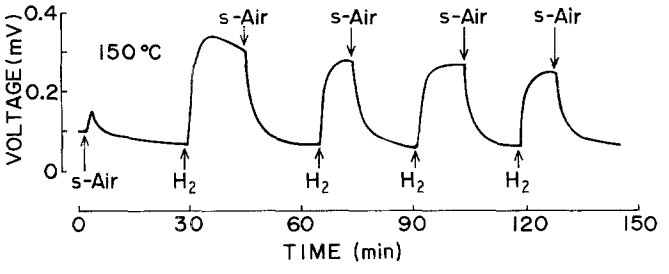

Figure 4 Response characteristics of a film sensor at 150° C. The film was sputtered for 3 min and annealed at 300° C for 2 h in air. The substrate is a sintered alumina. $d = 455 \pm 5\,\mu$m, $V_0 = 6$ V, $R_x = 1$ kΩ.

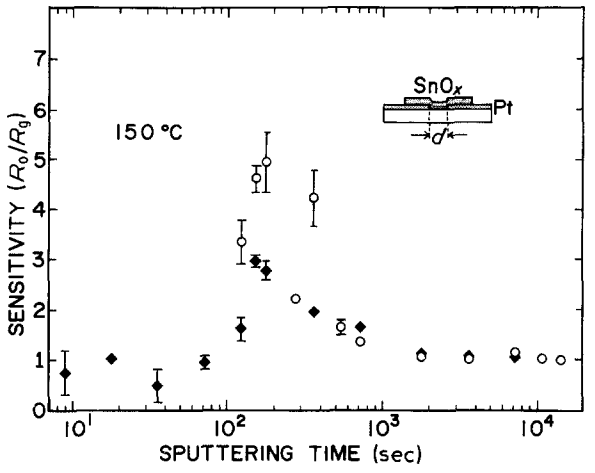

Figure 5 Sensitivities as a function of sputtering time. Deposition rate = 0.049 nm sec^{-1}. (○) d = 455 ± 5 μm, (◆) 80 ± 20 μm.

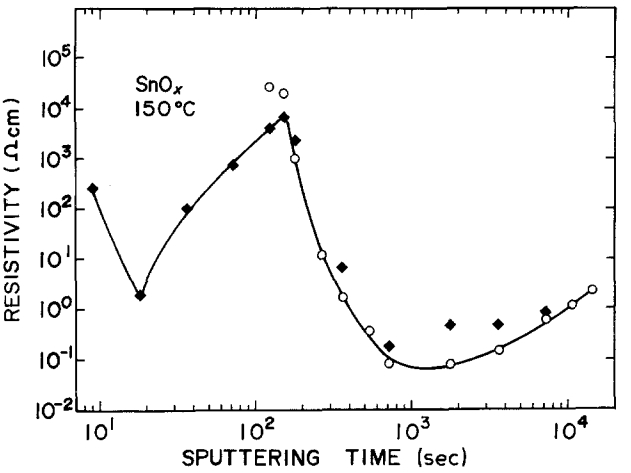

Figure 7 Resistivities as a function of sputtering time. Deposition rate = 0.049 nm sec^{-1}. Electrode gap: (○) 455 ± 5 μm, (◆) 80 ± 20 μm.

lower current density of the order of 1 mA cm^{-2}. The sudden jump in resistivity in the 9 sec film may be due to the formation of an island structure. So far, our observations had been made on films deposited on sintered alumina substrates. Because the substrate can have a significant influence on the properties of the films [5, 11], films on other substrates were examined next.

3.4. Substrate

Fig. 8 shows the effects of five substrates on resistivity and sensitivity as a function of the thermal expansion coefficient. All films were deposited for 3 min (8.7 nm thick) on substrates having an electrode gap of 455 ± 5 μm. The thermal expansion coefficient of crystalline SnO_2 is reported to be 5 × 10^{-6} °C^{-1} [15]. As amorphous phases generally have smaller expansion coefficient than their crystalline counterparts, the expansion coefficient of an amorphous SnO_x may be situated near the Pyrex glass or lower. The figure indicates a higher resistivity with an increase of the expansion coefficient of the substrate. However, we see no correlation between sensitivity and expansion coefficient. This means that the surface state of the substrate plays an overwhelmingly important role on the sensitivity of ultrathin amorphous films. It is suspected that film properties demonstrated hitherto are not due solely to the thickness, but due to a complex interaction between thin amorphous films and sintered alumina substrates.

4. Conclusions

1. Ion-beam sputtering from an SnO_2 target has been successfully employed to deposit thin films on sintered alumina substrates.

2. Films ranging from ~ 1 to 700 nm were annealed at 300° C for 2 h in air. Film structure was found to be almost amorphous; a small amount of trigonal Sn_3O_4 phase was present in the film.

3. Thin films showed a strong thickness dependence of hydrogen sensitivity around the thickness of 10 nm.

4. The sensitivity of thin films also depended on the electrode gap; a wider gap showed a higher sensitivity.

5. Films showed a resistivity maximum at the thickness of 7.4 nm. Resistivity increased by three orders of magnitude with the increase of film thickness from 0.9 to 7.4 nm and then decreased by five orders of magnitude from 7.4 to 35 nm.

6. Sensitivity and resistivity of thin films were significantly influenced by the thermal expansion coefficient and the surface state of the substrate. A higher thermal expansion coefficient of the substrate resulted in a higher resistivity of the film.

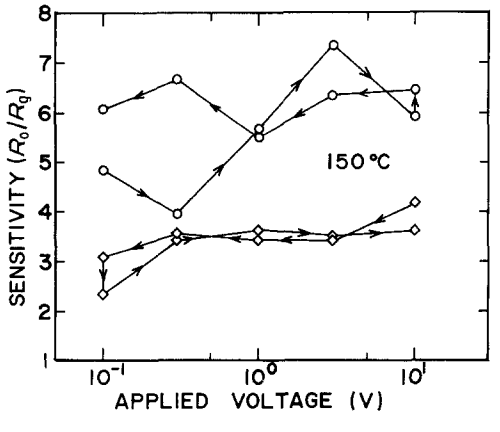

Figure 6 Sensitivities as a function of applied voltage. Films were sputtered for 3 min. (○) d = 455 ± 5 μm, (◇) d = 80 ± 20 μm.

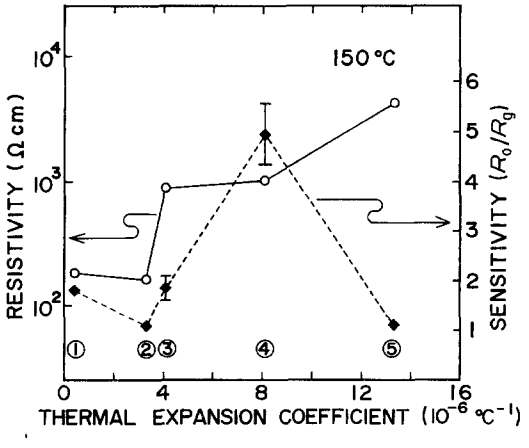

Figure 8 Effect of substrate on sensor properties. Films were sputtered for 3 min. The electrode gap is 455 ± 5 μm. Substrate: (1) quartz glass, (2) Pyrex glass, (3) mullite, (4) alumina, (5) magnesia.

Acknowledgement

We would like to thank Professor N. Oyama of the Department of Applied Chemistry for Resources for help in film thickness analysis.

References

1. T. SEIYAMA, A. KATO, K. FUJIISHI and M. NAGATANI, *Anal. Chem.* **34** (1962) 1502.
2. S. SAKAI, M. NAKAGAWA, I. DOI and M. MITSUDO, *Denkigakkai Denshisouchi Kenkyuukai Shiryou* EDD-75-50 (1975).
3. J. L. VOSSEN and E. S. POLINIAK, *Thin Solid Films* **13** (1972) 281.
4. H. PINK, L. TREITINGER and L. VITÉ, *Jpn J. Appl. Phys.* **19** (1980) 513.
5. H. KANEKO and K. MIYAKE, *J. Appl. Phys.* **53** (1982) 3629.
6. D. BELANGER, J. P. DODELET, B. A. LOMBOS and J. I. DICKSON, *J. Electrochem. Soc.* **132** (1985) 1398.
7. U. DIBBERN, G. KÜRSTEN and P. WILLICH, in "Proceedings of the 2nd International Meeting on Chemical Sensors, Bordeau, July, 1986", edited by J. L. Aucouturier, L. S. Cauhapé, M. Destriau, P. Hagenmuller, C. Lucat, F. Ménil, J. Portier and J. Salardenne (University of Bordeau, 1986) p. 127.
8. A. GRISEL and V. DEMARNE, *ibid.*, p. 247.
9. M. EGASHIRA, T. MATSUMOTO, H. KATSUKI and H. IWANAGA, *ibid.*, p. 213.
10. H. OGAWA, A. ABE, M. NISHIKAWA and S. HAYAKAWA, *J. Electrochem. Soc.* **128** (1981) 2020.
11. K. L. CHOPRA, S. MAJOR and D. K. PANDYA, *Thin Solid Films* **102** (1983) 1.
12. T. SUZUKI, T. YAMAZAKI, H. YOSHIOKA, K. TAKAHASHI and T. KAGEYAMA, *J. Mater. Sci. Lett.* **6** (1987) 437.
13. R. N. BLUMENTAL and M. A. SEITZ, "Electrical Conductivity in Ceramics and Glass, Part A" (Marcel Dekker, New York, 1974) p. 35.
14. H. K. HENISH, "Rectifying Semi-conductor Contacts" (Clarendon, Oxford, 1957) p. 221.
15. H. SEKI, N. ISHIZAWA, N. MIZUTANI and M. KATO, *Yogyo KyOkaishi* **92** (1984) 219.

Received 10 February
and accepted 29 April 1987